RSC Advances

PAPER

View Article Online
View Journal | View Issue

Cite this: *RSC Adv.*, 2020, **10**, 17266

Received 26th March 2020
Accepted 26th April 2020

DOI: 10.1039/d0ra02778b

rsc.li/rsc-advances

49.25% efficient cyan emissive sulfur dots *via* a microwave-assisted route†

Zhe Hu,[a] Hanqing Dai,[b] Xian Wei,[a] Danlu Su,[a] Chang Wei,[a] Yuanyuan Chen,[a] Fengxian Xie,[a] Wanlu Zhang,[a] Ruiqian Guo *[ab] and Songnan Qu*[c]

Cyan emissive sulfur dots with a record high photoluminescence (PL) quantum yield of 49.25% have been successfully prepared *via* a microwave-assisted top-down route. The PL enhancement induced by electrostatic repulsion of sulfite groups and steric hindrance of polyethylene glycol 400 (PEG-400) were investigated for the first time.

Introduction

Recently, luminescent quantum dots (QDs) with their size confined in three dimensions, have drawn tremendous attention in extensive potential applications, such as sensing, solar cells, bioimaging, catalysis and optoelectronic devices.[1–5] However, the toxicity of heavy-metal based QDs limits their wide-scale commercialization.[6–8] Hence, a great many efforts have been made to develop non-toxic QDs, especially pure element QDs such as carbon,[9] silicon,[10] sulfur[11] and phosphorus.[12] Additionally, the previous studies revealed that the pure element QDs possessed distinct benefits, such as chemical stability, good solubility and biocompatibility, making them the new-generation luminescent nanomaterials.[13–16] Moreover, sulfur dots (SDs) are superior to conventionally used QDs mentioned above due to their inherent antibacterial properties.[17]

Now, several efforts are focused on improving the photoluminescence properties of the SDs. For example, Li *et al.* firstly developed a facile phase interfacial reaction method for synthesizing blue emissive SDs with a photoluminescence quantum yield (PL QY) of only 0.549% through further converting CdS QDs into SDs by using HNO_3.[10] Then, Shen's group creatively proposed a top-down method by simply treating bulk sulfur powder with alkali *via* an "assemble-fission" reaction. Unfortunately, the PL QY of blue emission at 440 nm was barely up to 3.8% after 125 h treatment.[18] Subsequently, Wang and co-workers developed an H_2O_2-assisted top-down approach to synthesize tunable emissive SDs, which can cover from 440 to 500 nm by varying the concentration of H_2O_2, but the maximum PL QY of merely 23% is far lower than the actual application requirements.[19] Therefore, the research and development of highly luminescent SDs have a long-term significance for practical application.

Herein, we proposed a new strategy of realizing luminescent SDs with a record high PLQY of 49.25% *via* one-pot microwave-assisted top-down route. And the colour emission can be tuned from 445 to 506 nm. The results illustrated that the bulk sulfur powder was slowly dissolved into small particles in an alkaline environment, and the presence of polyethylene glycol 400 (PEG-400) played a key role in solubilization and passivation. Furthermore, the microwave irradiation with the rapid and equal heat at a certain temperature ensured increasing nucleation rate and adsorbing more sulfite groups. The electrostatic repulsion of abundant sulfite groups and the surface passivation by PEG-400 and H_2O_2 solution resulted in relatively excellent photoluminescence. Hence, these results imply that the outstanding luminescent SDs have great potential in practical application.

Experimental section

Sublimed sulfur (99.95%) and H_2O_2 were purchased form Sinopharm Chemical Reagent Co. Ltd. NaOH (96.0%) and polyethylene glycol 400 (PEG-400) were purchased from Shanghai Dahe Chemical Reagent Co. Ltd. All chemicals were used directly and without further purification.

The obtained samples were characterized by high-resolution transmission electron microscopy (HRTEM; Tecnai G2 F30, FEI, USA), X-ray photoelectron spectroscopy (XPS; Thermo Fisher Scientific K-Alpha, USA), and Fourier transform-infrared spectroscopy (FT-IR; PerkinElmer Spectrometer Frontier, USA). UV-vis absorption spectra and PL spectra of QDs were recorded using a UV-vis spectrophotometer (759S, Shanghai Lengguang,

[a]*Engineering Research Center of Advanced Lighting Technology, Ministry of Education, Institute for Electric Light Sources, Fudan University, Shanghai 200433, China. E-mail: rqguo@fudan.edu.cn*

[b]*Institute of Future Lighting, Academy for Engineering and Technology, Fudan University, Shanghai 200433, China*

[c]*Joint Key Laboratory of the Ministry of Education, Institute of Applied Physics and Materials Engineering, University of Macau, Avenida da Universidade, Taipa, Macau 999078, P. R. China. E-mail: qusn@ciomp.ac.cn*

† Electronic supplementary information (ESI) available. See DOI: 10.1039/d0ra02778b

China) and fluorescence spectrophotometer (F97XP, Shanghai Lengguang, China), respectively. The absolute PL QY and the PL decay curves were measured on a time-resolved spectrofluorometer (FL 3, HORIBA, France).

SDs were prepared in aqueous solution through a microwave-assisted approach. In detail, sulfur powder (1.4 g) and PEG-400 (3 mL) were mixed with 50 mL NaOH aqueous solution (80 mg mL^{-1}), vigorously stirred for 1 h and then heated to 70 °C, 80 °C, 90 °C and 95 °C, respectively *via* microwave irradiation within 5 min. After that, the solution was kept at the above four different temperatures for 30 min for the formation of the sulfur core. And then the solution was kept at 70 °C for a period of time (5 to 55 h) for the further growth of the core.

Results and discussion

From Fig. 1a and S1,† it can be seen that the fluorescence intensity is greatly promoted by increasing heating time. However, as the heating time exceeds about 40 h, the PL enhancement becomes less obvious. As shown in Fig. 1b, with the increase of the nucleation temperature, the emission peak intensity firstly increases and then decreases, presenting a maximum at 90 °C. And it should be noted that only the sample with the nucleation temperature at 90 °C is capable of emitting strong PL. Because of the rapidness and high-efficiency of microwave heating, SDs could emit PL within 30 h, which is superior to previous report.[18] Fig. 1c shows that the emission wavelengths of the SDs shift towards longer wavelength (from 445 to 506 nm) when the excitation wavelength varied from 360 to 440 nm, indicating that SDs exhibit excitation-dependent emission properties. This could be attributed to the quantum size effect of the SDs with the inhomogeneous size distribution[9] and the presence of multiple discrete electronic states.[20]

Fig. 1d shows the UV-vis absorption spectra of the SDs diluted 1000 times and 10 000 times (inset). For 5 h sample under 90 °C, three absorption bands centered at 216 nm (band 1), 298 nm (band 2) and 370 nm (band 3) can be recognized, which are usually assigned to the n → σ* transition of nonbonding electrons of S, S_2^{2-} and S_8^{2-} species adsorbed on the surface of the SDs, respectively.[10,21] The absorption bands of the SDs with nucleation temperatures at 70 °C, 80 °C and 95 °C were also recorded (Fig. S2†) and it can be seen that the absorption peaks position do not shift with increasing the heating time from 5 to 40 h. For the case of the SDs under 90 °C, however, it is highly worth noting that band 2 disappeared when the heating time was up to 25 h. In the meantime, a new band emerged at 330 nm, as shown in Fig. 1d (inset). Obviously, the emergence of the peak at around 330 nm is the key factor related to enhanced PL emission,[22] although the origin of this band is still an open question.

In addition to the optical properties discussed above, the morphologies of the SDs were characterized using transmission electron microscopy (TEM) and high-resolution TEM (HRTEM). Fig. 2a–c show the TEM image of the SDs obtained under different heating time. It is found that the size of the SDs decreased in the order of 4.00, 3.78 and 3.58 nm with the increased heating time. The HRTEM images in Fig. 2e and f reveal the high crystallinity and also show the clear lattice fringes of 0.23 nm. Such interplanar distance would be assigned to (3 3 7) crystal face and it was consistent with previous work.[23] Further analysis of TEM images (Fig. S3†) indicates that the as-synthesized 25 h and 40 h samples have more excellent monodispersibility than the 5 h sample.

To investigate the chemical composition of the SDs, X-ray photoelectron spectroscopy (XPS) was employed to characterize the surface group. Fig. 3a shows the XPS full survey of the SDs which are mainly composed of C, O and S elements. Moreover, the relative content of elemental oxygen is much higher than that of previous studies[18] and this is because of the high surface-to-volume ratio of the SDs. On the basis of our findings, it can be concluded that the microwave-assisted

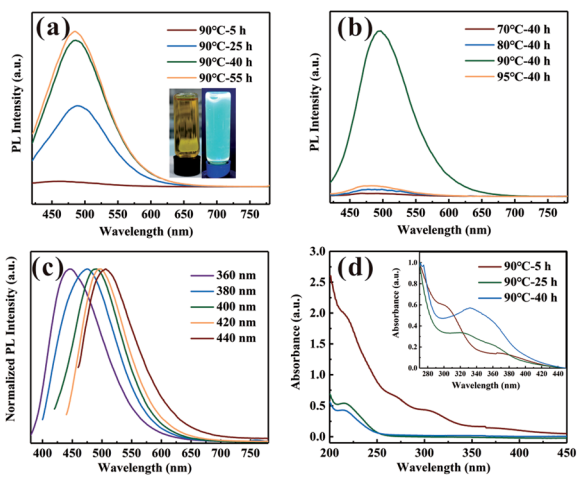

Fig. 1 (a) PL spectra of the SDs under the nucleation temperature of 90 °C for different heating time and photographs (inset) of the SDs in daylight (left) and irradiated by UV light at 365 nm (right). (b) PL spectra of the SDs under different nucleation temperatures for 40 h. (c) PL spectra of the SDs under 90 °C for 40 h irradiated by different excitation wavelengths. (d) UV-vis absorption spectra of the SDs under 90 °C diluted 1000 times and 10 000 times (inset) at different heating times.

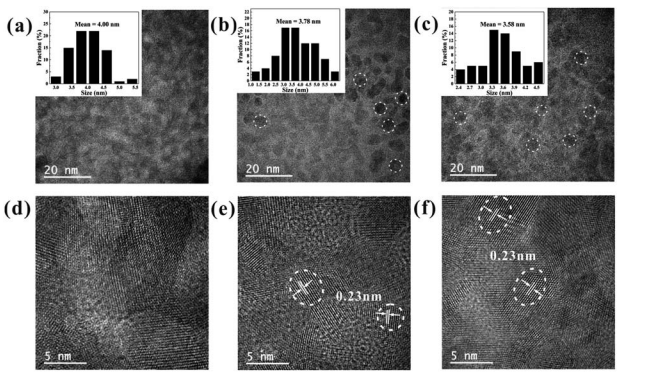

Fig. 2 TEM (inset: size distribution) and high-resolution TEM (HRTEM) images of the SDs under 90 °C at (a) and (d) 5 h; (b) and (e) 25 h and (c) and (f) 40 h.

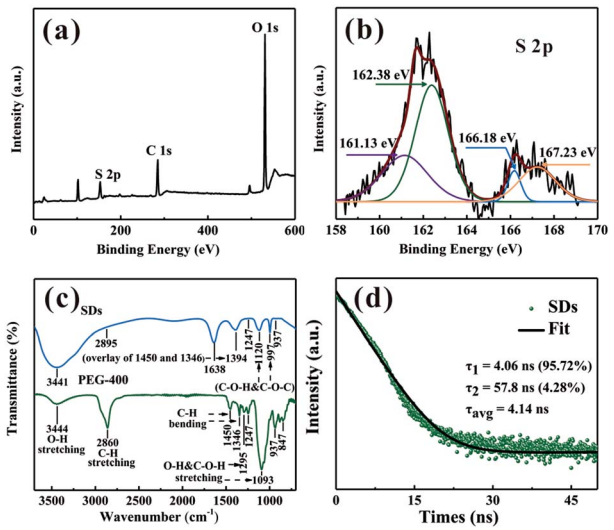

Fig. 3 (a) XPS survey and (b) high-resolution S 2p peaks of the SDs under 90 °C for 40 h. (c) FT-IR spectra of the PEG-400 and SDs under 90 °C for 40 h. (d) Time-resolved PL decay curve of the SDs under 90 °C for 40 h.

heating at 90 °C induces growing more sulfur cores so that they could adsorb more sulfite groups. According to the high-resolution XPS spectrum of S 2p in Fig. 3b, there are four peaks. Two peaks appeared at 161.13 eV and 162.38 eV are attributed to the atomic sulfur. The binding energies at 166.18 eV and 167.23 eV can be assigned to SO_2^{2-} ($2p_{2/3}$) and SO_3^{2-} ($2p_{2/3}$).[21] Thus, we concluded that the SDs were mainly composed of atomic sulfur and abundant sulfite groups on the surface. It is worth noting that the as-prepared sample is incapable of emitting PL without PEG-400 as surface passivation agent, which demonstrates that the presence of PEG-400 is crucial. Furthermore, the surface-related functional groups of the SDs and PEG-400 were detected by Fourier transform infrared (FT-IR) spectra (Fig. 3c). In FT-IR spectra, the absorption bands at around 3441, 2895, 1247 and 937 cm^{-1} are observed in both of two samples. Besides, the new peaks of the SDs are split up or overlapped into other characteristic peaks of PEG-400 including the bending vibrations of C–H (1450 and 1346 cm^{-1}) and the stretching vibrations of O–H or C–O–H (1295 and 1093 cm^{-1}). The FT-IR results demonstrate that there is no chemical interaction between PEG-400 and SDs.

The time-resolved PL decay for the emission at 490 nm was further measured to get specific information about dynamical features. From Fig. 3d, the decay curve of the SDs can be well fitted by the following bi-exponential function: $f(\tau) = A_1 \exp(-\tau/\tau_1) + A_2 \exp(-\tau/\tau_2)$. The average lifetime of the SDs is 4.14 ns and the biexponential decay behaviour strongly suggests that two different species are involved in the emission. A short-lived component τ_1 and a long-lived component τ_2 indicate the strong coupling between the core states and the surface states similar to the carbon dots.[24,25] It can be deduced that the intrinsic state is attributed to the sulfur core and it occupies a dominant position. Although the nonradiative surface defects were partially eliminated in the presence of PEG-400, the absolute PL QY of the cyan emissive SDs is as high as 42.95% when excited at 400 nm.

The bulk sulfur can be dissolved at alkaline pH by the solubilization effect of the PEG-400, as shown in reaction (1). Next, the generated sodium sulfide reacted with sulfur powder to form sodium polysulfide (reaction (2)). The inhomogeneous sodium polysulfide particles have high surface energy and the PEG-400 physically adsorbed on the surface tried to prevent the aggregation. However, the steric hindrance effect of the PEG-400 is too weak to restrain the aggregation of the particles.

$$3S + 6NaOH = 2Na_2S + Na_2SO_3 + 3H_2O \quad (1)$$

$$(x - 1)S + Na_2S = Na_2S_x \quad (2)$$

To disperse the particles, the pretreatment with microwave-assisted heating at 90 °C is utilized to grow more sulfur cores. When the temperature was rapidly raised to 90 °C within 5 min, the higher temperature ensured that the activated energy barrier of the nucleation could be overcome. It increased the nucleation rate and thus more sulfite groups with negative charges could be attracted onto the surface of the sulfur core. The abundant sulfite groups repelled each other with a large repulsion, which enhanced the fission effect (Fig. 4). The excellent dispersing performance of the SDs is owing to the co-action of electrostatic repulsion of sulfite groups and steric hindrance of the PEG-400.

Similar to carbon and silicon QDs, the PL from the SDs might be attributed to the presence of surface energy traps that become emissive upon stabilization as a result of the surface passivation.[9] In this work, PEG-400 attached to the surface can also effectively eliminate surface defects, which can prominently improve the PL of the SDs. Based on the PL lifetime data, surface defects were not entirely passivated. Therefore, similar to Wang's method,[19] 3 wt% H_2O_2 solution was mixed with the SDs and further ensured the etching of the surface. A shorter average PL lifetime was observed for the SDs as compared with that of the untreated SDs, indicating a lower amount of surface states in the former (Fig. S4†).[19] The PL of the SDs can be further enhanced (Fig. S5†) and the PL QY of the SDs also increases from 42.95% to 49.25%.

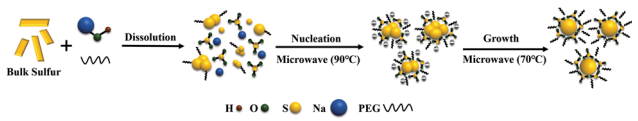

Fig. 4 A possible growth mechanism for the SDs.

Conclusions

In summary, microwave-assisted top-down method for the preparation of cyan emissive SDs with a record high PL QY of 49.25% is reported in this work. The dramatic enhancement of the PL QY lies in the fact that the aggregation in the SDs has been effectively avoided through electrostatic repulsion of sulfite groups and steric hindrance of PEG-400. The co-action of

PEG-400 and H_2O_2 by eliminating surface traps further improves the PL QY of the SDs. In general, SDs are deemed to have promising potential applications due to their low toxicity, good water-solubility, biocompatibility and antibacterial activity. Moreover, the proposed strategy will promote the exploration and application of the SDs.

Conflicts of interest

There are no conflicts to declare.

Acknowledgements

This work was supported by the National Natural Science Foundation of China (NSFC, No. 61675049 and NSFC, No. 61377046) and Fudan University – CIOMP Joint Fund (FC2017-004) and Zhongshan – Fudan Joint Innovation Center.

Notes and references

1 X. Michalet, F. F. Pinaud, L. A. Bentolila, J. M. Tsay, S. Doose, J. J. Li, G. Sundaresan, A. M. Wu, S. S. Gambhir and S. Weiss, *Science*, 2005, **307**, 538–544.
2 L. Jing, S. V. Kershaw, Y. Li, X. Huang, Y. Li, A. L. Rogach and M. Gao, *Chem. Rev.*, 2016, **116**, 10623–10730.
3 S. Mei, X. Wei, Z. Hu, C. Wei, D. Su, D. Yang, G. Zhang, W. Zhang and R. Guo, *Opt. Mater.*, 2019, **89**, 224–230.
4 S. Qu, D. Zhou, D. Li, W. Ji, P. Jing, D. Han, L. Liu, H. Zeng and D. Shen, *Adv. Mater.*, 2016, **28**, 3516–3521.
5 W. Zhu, Y. Zhao, J. Duan, Y. Duan, Q. Tang and B. He, *Chem. Commun.*, 2017, **53**, 9894–9897.
6 J. Hu, Z.-y. Wang, C.-c. Li and C.-y. Zhang, *Chem. Commun.*, 2017, **53**, 13284–13295.
7 G. Xu, S. Zeng, B. Zhang, M. T. Swihart, K.-T. Yong and P. N. Prasad, *Chem. Rev.*, 2016, **116**, 12234–12327.
8 C. Coughlan, M. Ibanez, O. Dobrozhan, A. Singh, A. Cabot and K. M. Ryan, *Chem. Rev.*, 2017, **117**, 5865–6109.
9 Y. P. Sun, B. Zhou, Y. Lin, W. Wang, K. A. S. Fernando, P. Pathak, M. J. Meziani, B. A. Harruff, X. Wang, H. F. Wang, P. J. G. Luo, H. Yang, M. E. Kose, B. L. Chen, L. M. Veca and S. Y. Xie, *J. Am. Chem. Soc.*, 2006, **128**, 7756–7757.
10 S. Li, D. Chen, F. Zheng, H. Zhou, S. Jiang and Y. Wu, *Adv. Funct. Mater.*, 2014, **24**, 7133–7138.
11 Y. He, Y. Su, X. Yang, Z. Kang, T. Xu, R. Zhang, C. Fan and S.-T. Lee, *J. Am. Chem. Soc.*, 2009, **131**, 4434–4438.
12 X. Zhang, H. Xie, Z. Liu, C. Tan, Z. Luo, H. Li, J. Lin, L. Sun, W. Chen, Z. Xu, L. Xie, W. Huang and H. Zhang, *Angew. Chem., Int. Ed.*, 2015, **54**, 3653–3657.
13 M. Montalti, A. Cantelli and G. Battistelli, *Chem. Soc. Rev.*, 2015, **44**, 4853–4921.
14 D. Zhou, D. Li, P. Jing, Y. Zhai, D. Shen, S. Qu and A. L. Rogach, *Chem. Mater.*, 2017, **29**, 1779–1787.
15 Z. Bai, W. Ji, D. Han, L. Chen, B. Chen, H. Shen, B. Zou and H. Zhong, *Chem. Mater.*, 2016, **28**, 1085–1091.
16 Y. Ye, F. Wu, S. Xu, W. Qu, L. Li and R. Chen, *J. Phys. Chem. Lett.*, 2018, **9**, 1398–1414.
17 J. Lim, J. Pyun and K. Char, *Angew. Chem., Int. Ed.*, 2015, **54**, 3249–3258.
18 L. Shen, H. Wang, S. Liu, Z. Bai, S. Zhang, X. Zhang and C. Zhang, *J. Am. Chem. Soc.*, 2018, **140**, 7878–7884.
19 H. Wang, Z. Wang, Y. Xiong, S. V. Kershaw, T. Li, Y. Wang, Y. Zhai and A. L. Rogach, *Angew. Chem., Int. Ed.*, 2019, **58**, 7040–7044.
20 A. Sharma, T. Gadly, A. Gupta, A. Ballal, S. K. Ghosh and M. Kumbhakar, *J. Phys. Chem. Lett.*, 2016, **7**, 3695–3702.
21 N. S. Manan, L. Aldous, Y. Alias, P. Murray, L. J. Yellowlees, M. C. Lagunas and C. Hardacre, *J. Phys. Chem. B*, 2011, **115**, 13873–13879.
22 Z. Wang, C. Zhang, H. Wang, Y. Xiong, X. Yang, Y. Shi and A. L. Rogach, *Angew. Chem., Int. Ed.*, 2020, **132**, 1–7.
23 G. Qiao, L. Liu, X. Hao, L. Zheng, W. Liu, J. Gao, C. Zhang and Q. Wang, *Chem. Eng. J.*, 2020, **382**, 122907.
24 Y. Zhang, R. Yuan, M. He, G. Hu, J. Jiang, T. Xu, L. Zhou, W. Chen, W. Xiang and X. Liang, *Nanoscale*, 2017, **9**, 17849–17858.
25 L. Ma, W. Xiang, H. Gao, L. Pei, X. Ma, Y. Huang and X. Liang, *J. Mater. Chem. C*, 2015, **3**, 6764–6770.